

# Polyphonic Sound Event Detection by using Capsule Neural Networks

Fabio Vesperini\*, Leonardo Gabrielli, Emanuele Principi, and Stefano Squartini, *Senior Member, IEEE*

**Abstract**—Artificial sound event detection (SED) has the aim to mimic the human ability to perceive and understand what is happening in the surroundings. Nowadays, Deep Learning offers valuable techniques for this goal such as Convolutional Neural Networks (CNNs). The Capsule Neural Network (CapsNet) architecture has been recently introduced in the image processing field with the intent to overcome some of the known limitations of CNNs, specifically regarding the scarce robustness to affine transformations (i.e., perspective, size, orientation) and the detection of overlapped images. This motivated the authors to employ CapsNets to deal with the polyphonic-SED task, in which multiple sound events occur simultaneously. Specifically, we propose to exploit the capsule units to represent a set of distinctive properties for each individual sound event. Capsule units are connected through a so-called *dynamic routing* that encourages learning part-whole relationships and improves the detection performance in a polyphonic context. This paper reports extensive evaluations carried out on three publicly available datasets, showing how the CapsNet-based algorithm not only outperforms standard CNNs but also allows to achieve the best results with respect to the state of the art algorithms.

**Index Terms**—Capsule Neural Networks, Convolutional Neural Network, Polyphonic Sound Event Detection, DCASE, Computational Audio Processing

## I. INTRODUCTION

HUMAN cognition relies on the ability to sense, process, and understand the surrounding environment and its sounds. Although the skill of listening and understanding their origin is so natural for living beings, it still results in a very challenging task for computers.

Sound event detection (SED), or acoustic event detection, has the aim to mimic this cognitive feature by means of artificial systems. Basically, a SED algorithm is designed to detect the onset and offset times for a variety of sound events captured in an audio recording and associate a textual descriptor, i.e., a label for each of these events.

In recent years, SED has received the interest from the computational auditory scene analysis community [1], due to its potential in several engineering applications. Indeed, the automatic recognition of sound events and scenes can have a considerable impact in a wide range of applications where sound or sound sensing is advantageous with respect to other modalities. This is the case of acoustic surveillance [2], healthcare monitoring [3], [4] or urban sound analysis [5], where the short duration of certain events (i.e., a human fall, a gunshot or a glass breaking) or the personal privacy motivate

the exploitation of the audio information rather than, e.g., the image processing. In addition, audio processing is often less computationally demanding compared to other multimedia domains, thus embedded devices can be easily equipped with microphones and sufficient computational capacity to locally process the signal captured. These could be smart home devices for home automation purposes or sensors for wildlife and biodiversity monitoring (i.e., bird calls detection [6]).

SED algorithms in a real-life scenario face many challenges. These include simultaneous events, environmental noise and events of the same class produced by different sources [7]. Since multiple events are very likely to overlap, a *polyphonic* SED algorithm, i.e., an algorithm able to detect multiple simultaneous events, needs to be designed. Finally, the effects of noise and intra-class variability represent further challenges for SED in real-life situations.

Traditionally, the polyphonic acoustic event analysis has been approached with statistical modelling methods, including Hidden Markov Models (HMM) [8], Gaussian Mixture Models (GMM) [9], Non-negative Matrix Factorization (NMF) [10] and support vector machines (SVM) [11]. In the recent era of the “Deep Learning”, different neural network architectures have been successfully used for sound event detection and classification tasks, including feed-forward neural networks (FNN) [12], deep belief networks [13], convolutional neural networks (CNNs) [14] and Recurrent Neural Networks (RNNs) [15]. In addition, these architectures laid the foundation for end-to-end systems [16], [17], in which the feature representation of the audio input is automatically learnt from the raw audio signal waveforms.

### A. Related Works

The use of deep learning models has been motivated by the increased availability of datasets and computational resources and resulted in significant performance improvements. The methods based on CNNs and RNNs have established the new state-of-the-art performance on the SED task, thanks to the capabilities to learn the non-linear relationship between time-frequency features of the audio signal and a target vector representing sound events. In [18], the authors show how “local” patterns can be learned by a CNN and can be exploited to improve the performance of detection and classification of non-speech acoustic events occurring in conversation scenes, in particular compared to a FNN-based system which processes multiple resolution spectrograms in parallel.

The combination of the CNN structure with recurrent units has increased the detection performance by taking advantage

\*Corresponding author.

The authors are with the A3lab, Department of Information Engineering, Università Politecnica delle Marche, Ancona (Italy), E-mail: f.vesperini@pm.univpm.it, {l.gabrielli,e.principi,s.squartini}@univpm.it

of the characteristics of each architecture. This is the case of convolutional recurrent neural networks (CRNNs) [19], which provided state-of-the-art performance especially in the case of polyphonic SED. CRNNs consolidate the CNN property of local shift invariance with the capability to model short and long term temporal dependencies provided by the RNN layers. This architecture has been also employed in almost all of the most performing algorithms proposed in the recent editions of research challenges such as the IEEE Audio and Acoustic Signal Processing (AASP) Challenge on Detection and Classification of Acoustic Scenes and Events (DCASE) [20]. On the other hand, if the datasets are not sufficiently large, problems such as overfitting can be encountered with these models, which typically are composed of a considerable number of free-parameters (i.e., more than 1M).

Encouraging polyphonic SED performance have been obtained using CapsNets in preliminary experiments conducted on the Bird Audio Detection task in occasion of the DCASE 2018 challenge [21], confirmed by the results reported in [22]. The CapsNet [23] is a recently proposed architecture for image classification and it is based on the grouping of activation units into novel structures introduced in [24], named *capsules*, along with a procedure called dynamic routing. The capsule has been designed to represent a set of properties for an entity of interest, while dynamic routing is included to allow the network to implicitly learn global coherence and to identify part-whole relationships between capsules.

The authors of [23] show that CapsNets outperform state-of-the-art approaches based on CNNs for digit recognition in the MNIST dataset case study. They designed the CapsNet to learn how to assign the suited partial information to the entities that the neural network has to predict in the final classification. This property should overcome the limitations of solutions such as max-pooling, currently employed in CNNs to provide local translation invariance, but often reported to cause an excessive information loss. Theoretically, the introduction of the dynamic routing can supply invariances for any property captured by a capsule, allowing also to adequately train the model without requiring extensive data augmentation or dedicated domain adaptation procedures.

### B. Contribution

The proposed system is a fully data-driven approach based on the CapsNet deep neural architecture presented by Sabour et al. [23]. This architecture has shown promising results on highly overlapped digital numbers classification. In the audio field, a similar condition can be found in the detection of multiple concomitant sound events from acoustic spectral representations, thereby we propose to employ the CapsNet for the polyphonic-SED in real-life recordings. The novel computational structure based on capsules, combined to the routing mechanism allows to be invariant to intra-class affine transformations and to identify part-whole relationships between data features. In the SED case study, it is hypothesized that this characteristic confers to CapsNet the ability to effectively select most representative spectral features of each individual sound event and separate them from overlapped descriptions of the other sounds in the mixture.

This hypothesis is supported by previously mentioned related works. Specifically, in [21], the CapsNet is exploited in order to obtain the prediction of the presence of heterogeneous polyphonic sounds (i.e., bird calls) on unseen audio files recorded in various conditions. In [22] the dynamic routing yields promising results for SED with a *weakly labeled* training dataset, thus with unavailable ground truths for the onset and offset times of the sound events. The algorithm has to detect sound events without supervision and in this context the routing can be considered as an attention mechanism.

In this paper, we present an extensive analysis of SED conducted on real-life audio datasets and compare the results with state-of-the-art methods. In addition, we propose a variant of the dynamic routing procedure which takes into account the temporal dependence of adjacent frames. The proposed method outperforms previous SED approaches in terms of detection error rate in the case of polyphonic SED, while it has comparable performance with respect to CNNs in the case of monophonic SED.

The whole system is composed of a feature extraction stage and a detection stage. The feature extraction stage transforms the audio signal into acoustic spectral features, while the second stage processes these features to detect the onset and offset times of specific sound events. In this latter stage we include the capsule units. The network parameters are obtained by supervised learning using annotations of sound events activity as target vectors. We have evaluated the proposed method against three datasets of real-life recordings and we have compared its performance both with the results of experiments with a traditional CNN architecture, and with the performance of well-established algorithms which have been assessed on the same datasets.

The rest of the paper is organized as follows. In Section II the task of polyphonic SED is formally described and the stages of the approach we propose are detailed, including a presentation of the CapsNet architecture characteristics. In Section III, we present the evaluation set-up used to accomplish the performance of the algorithm we propose and the comparative methods. In Section IV the results of experiments are discussed and compared with baseline methods. Section V finally presents our conclusions for this work.

## II. PROPOSED METHOD

The aim of polyphonic SED is to find and classify any sound event present in an audio signal. The algorithm we propose is composed of two main stages: sound representation and polyphonic detection. In the sound representation stage, the audio signal is transformed in a two-dimensional time-frequency representation to obtain, for each frame  $t$  of the audio signal, a feature vector  $\mathbf{x}_t \in \mathbb{R}^F$ , where  $F$  represents the number of frequency bands.

Sound events possess temporal characteristics that can be exploited for SED, thus certain events can be efficiently distinguished by their time evolution. Impulsive sounds are extremely compact in time (e.g., gunshot, object impact), while other sound events have indefinite length (i.e., wind blowing, people walking). Other events can be distinguished

from their spectral evolution (e.g., bird singing, car passing by). Long-term time domain information is very beneficial for SED and motivates for the use of a temporal *context* allowing the algorithm to extract information from a chronological sequence of input features. Consequently, these are presented as a context window matrix  $\mathbf{X}_{t:t+T-1} \in \mathbb{R}^{T \times F \times C}$ , where  $T \in \mathbb{N}$  is the number of frames that defines the sequence length of the temporal context,  $F \in \mathbb{N}$  is the number of frequency bands and  $C$  is the number of audio channels. Differently, the target output matrix is defined as  $\mathbf{Y}_{t:t+T-1} \in \mathbb{N}^{T \times K}$ , where  $K$  is the number of sound event classes.

In the SED stage, the task is to estimate the probabilities  $p(\mathbf{Y}_{t:t+T-1} | \mathbf{X}_{t:t+T-1}, \theta) \in \mathbb{R}^{T \times K}$ , where  $\theta$  denotes the parameters of the neural network. The network outputs, i.e., the event activity probabilities, are then compared with a threshold in order to obtain event activity predictions  $\hat{\mathbf{Y}}_{t:t+T-1} \in \mathbb{N}^{T \times K}$ . The parameters  $\theta$  are trained by supervised learning, using the frame-based annotation of the sound event class as target output, thus, if class  $k$  is active during frame  $t$ ,  $Y(t, k)$  is equal to 1, and is set to 0 otherwise. The case of polyphonic SED implies that this target output matrix can have multiple non-zero elements  $K$  in the same frame  $t$ , since several classes can be simultaneously present.

Indeed, polyphonic SED can be formulated as a multi-label classification problem in which the sound event classes are detected by multi-label annotations over consecutive time frames. The onset and offset time for each sound event are obtained by combining the classification results over consequent time frames. The trained model will then be used to predict the activity of the sound event classes in an audio stream without any further post-processing operations and prior knowledge on the events locations.

#### A. Feature Extraction

For our purpose, we exploit two acoustic spectral representation, the magnitude of the Short Time Fourier Transform (STFT) and the *LogMel* coefficients, obtained from all the audio channels and extensively used for other SED algorithms. Except where differently stated, we study the performance of binaural audio features and compare it with those extracted from a single channel audio signal. In all cases, we operate with audio signals sampled at 16 kHz and we calculate the STFT with a frame size equal to 40 ms and a frame step equal to 20 ms. Furthermore, the audio signals are normalized to the range  $[-1, 1]$  in order to have the same dynamic range for all the recordings.

The STFT is computed on 1024 points for each frame, while LogMel coefficients are obtained by filtering the STFT magnitude spectrum with a filter-bank composed of 40 filters evenly spaced in the mel frequency scale. In both cases, the logarithm of the energy of each frequency band is computed. The input matrix  $\mathbf{X}_{t:t+T-1}$  concatenates  $T = 256$  consequent STFT or LogMel vectors for each channel  $C = \{1, 2\}$ , thus the resulting feature tensor is  $\mathbf{X}_{t:t+T-1} \in \mathbb{R}^{256 \times F \times C}$ , where  $F$  is equal to 513 for the STFT and equal to 40 for the LogMels. The range of feature values is then normalized according to the mean and the standard deviation computed on the training sets of the neural networks.

#### B. CapsNet Architecture

The CapsNet architecture relies on the CNN architecture and includes its computational units in the first layers of the network as invariant features extractor from the input hereafter referred as  $\mathbf{X}$ , omitting the subscript  $t:t+T-1$  for simplicity of notation.

The essential unit of a CNN model is named *kernel* and it is composed of multiple neurons which process the whole input matrix by computing the linear convolution between the input and the kernel itself. The outputs of a CNN layer are called *feature maps*, and they represent translated replicas of high-level features. The feature maps are obtained by applying a non linear function to the sum of a bias term and the linear filtered version of the input data. Denoting with  $\mathbf{W}_m \in \mathbb{R}^{K_1^m \times K_2^m}$  the  $m$ -th kernel and with  $\mathbf{b}_m \in \mathbb{R}^{T \times F}$  the bias vector of a generic convolutional layer, the  $m$ -th feature map  $\mathbf{H}_m \in \mathbb{R}^{T \times F}$  is given by:

$$\mathbf{H}_m = \varphi(\mathbf{W}_m * \mathbf{X} + \mathbf{b}_m), \quad (1)$$

where  $*$  represents the convolution operation,  $\varphi(\cdot)$  the differentiable non-linear activation function. The coefficients of  $\mathbf{W}_m$  and  $\mathbf{b}_m$  are learned during the model training. The dimension of the  $m$ -th feature map  $\mathbf{H}_m$  depends on the zero padding of the input tensor: here, padding is performed in order to preserve the dimension of the input. Moreover, Eq. (1) is typically followed by a max-pooling layer, which in this case operates only on the frequency axis.

Following Hinton's preliminary works [24], in the CapsNet presented in [23] two layers are divided into many small groups of neurons called *capsules*. In those layers, the scalar-output feature detectors of CNNs are replaced with vector-output capsules and the dynamic routing, or *routing-by-agreement* algorithm is used in place of max-pooling, in order to replicate learned knowledge across space. Formally, we can rewrite Eq. (1) as

$$\mathbf{H}_m = \begin{bmatrix} \alpha_{11} \mathbf{W}_{11} \mathbf{X}_1 + \dots + \alpha_{M1} \mathbf{W}_{1M} \mathbf{X}_M \\ \vdots \\ \alpha_{1K} \mathbf{W}_{K1} \mathbf{X}_1 + \dots + \alpha_{MK} \mathbf{W}_{KM} \mathbf{X}_M \end{bmatrix}. \quad (2)$$

In Eq. (2),  $(\mathbf{W} * \mathbf{X})$  has been partitioned into  $K$  groups, or capsules, so that each row in the column vector corresponds to an output capsule (the bias term  $\mathbf{b}$  has been omitted for simplicity). Similarly,  $\mathbf{X}$  has been partitioned into  $M$  capsules, where  $\mathbf{X}_i$  denotes an input capsule  $i$ , and  $\mathbf{W}$  has been partitioned into submatrices  $\mathbf{W}_{ij}$  called *transformation matrices*. Conceptually, a capsule incorporates a set of properties of a particular entity that is present in the input data. With this purpose, coefficients  $\alpha_{ij}$  have been introduced. They are called *coupling coefficients* and if we set all the  $\alpha_{ij} = 1$ , Eq. (1) is obtained again.

The coefficients  $\alpha_{ij}$  affect the learning dynamics with the aim to represent the amount of agreement between an input capsule and an output capsule. In particular, they measure how likely capsule  $i$  may activate capsule  $j$ , so the value of  $\alpha_{ij}$  should be relatively accentuated if the properties of capsule  $i$  coincide with the properties of capsule  $j$  in the layer above. The coupling coefficients are calculated by the

iterative process of dynamic routing to fulfill the idea of assigning parts to wholes. Capsules in the higher layers should comprehend capsules in the layer below in terms of the entity they identify, while dynamic routing iteratively attempts to find these associations and supports capsules to learn features that ensure these connections.

In this work, we employ two layers composed of capsule units, and we denote them as Primary Capsules for the lower layer and Detection Capsules for the output layer throughout the rest of the paper.

1) *Dynamic Routing*: After giving a qualitative description of routing, we describe the method used in [23] to compute the coupling coefficients. The activation of a capsule unit is a vector which holds the properties of the entity it represents in its direction. The vector's magnitude indicates instead the probability that the entity represented by the capsule is present in the current input. To interpret the magnitude as a probability, a *squashing* non-linear function is used, which is given by:

$$\mathbf{v}_j = \frac{\|\mathbf{s}_j\|^2}{1 + \|\mathbf{s}_j\|^2} \frac{\mathbf{s}_j}{\|\mathbf{s}_j\|}, \quad (3)$$

where  $\mathbf{v}_j$  is the vector output of capsule  $j$  and  $\mathbf{s}_j$  is its total input.  $\mathbf{s}_j$  is a weighted sum over all the outputs  $\mathbf{u}_i$  of a capsule in the Primary Capsule layer multiplied by the coupling matrix  $\mathbf{W}_{ij}$ :

$$\mathbf{s}_j = \sum_i \alpha_{ij} \hat{\mathbf{u}}_{j|i}, \quad \hat{\mathbf{u}}_{j|i} = \mathbf{W}_{ij} \mathbf{u}_i. \quad (4)$$

The routing procedure work as follows. The coefficient  $\beta_{ij}$  measures the coupling between the  $i$ -th capsule from the Primary Capsule layer and the  $j$ -th capsule of the Detection Capsule layer. The  $\beta_{ij}$  are initialized to zero, then they are iteratively updated by measuring the agreement between the current output  $\mathbf{v}_j$  of each capsule in the layer  $j$  and the prediction  $\hat{\mathbf{u}}_{j|i}$  produced by the capsule  $i$  in the layer below. The agreement is computed as the scalar product

$$c_{ij} = \mathbf{v}_j \cdot \hat{\mathbf{u}}_{j|i}, \quad (5)$$

between the aforementioned capsule outputs. It is a measure of how similar the directions (i.e., the proprieties of the entity they represent) of capsules  $i$  and  $j$  are. The  $\beta_{ij}$  coefficients are treated as if they were log likelihoods, thus the agreement value is added to the value owned at previous routing step:

$$\beta_{ij}(r+1) = \beta_{ij}(r) + c_{ij}(r) = \beta_{ij}(r) + \mathbf{v}_j \cdot \hat{\mathbf{u}}_{j|i}(r), \quad (6)$$

where  $r$  represents the routing iteration. In this way the new values for all the coupling coefficients linking capsule  $i$  to higher level capsules are computed. To ensure that the coupling coefficients  $\alpha_{ij}$  represent log prior probabilities, the softmax function to  $\beta_{ij}$  is computed at the start of each new routing iteration. Formally:

$$\alpha_{ij} = \frac{\exp(\beta_{ij})}{\sum_k \exp(\beta_{ik})}, \quad (7)$$

so  $\sum_j \alpha_{ij} = 1$ . Thus,  $\alpha_{ij}$  can be seen as the probability that the entity represented by capsule Primary Capsule  $i$  is a part of the entity represented by the Detection Capsule  $j$  as opposed to any other capsule in the layer above.

2) *Margin loss function*: The length of the vector  $\mathbf{v}_j$  is used to represent the probability that the entity represented by the capsule  $j$  exists. The CapsNet have to be trained to produce long instantiation vector at the corresponding  $k_{th}$  capsule if the event that it represents is present in the input audio sequence. A separate margin loss is defined for each target class  $k$  as:

$$L_k = T_k \max(0, m^+ - \|\mathbf{v}_j\|)^2 + \lambda(1 - T_k) \max(0, \|\mathbf{v}_j\| - m^-)^2 \quad (8)$$

where  $T_k = 1$  if an event of class  $k$  is present, while  $\lambda$  is a down-weighting factor of the loss for absent sound event classes.  $m^+$ ,  $m^-$  and  $\lambda$  are respectively set equal to 0.9, 0.1 and 0.5 as suggested in [23]. The total loss is simply the sum of the losses of all the Detection Capsules.

### C. CapsNet for Polyphonic Sound Event Detection

The architecture of the neural network is shown in Fig. II-C. The first stages of the model are traditional CNN blocks which act as feature extractors on the input  $\mathbf{X}$ . After each block, max-pooling is used to halve the dimensions only on the frequency axis. The feature maps obtained by the CNN layers are then fed to the Primary Capsule Layer that represents the lowest level of multi-dimensional entities. Basically, it is a convolutional layer with  $J \cdot M$  filters, i.e., it contains  $M$  convolutional capsules with  $J$  kernels each. Its output is then reshaped and squashed using Eq. (3). The final layer, or Detection Capsule layer, is a time-distributed capsule layer (i.e., it applies the same weights and biases to each frame element) and it is composed of  $K$  densely connected capsule units of dimension  $G$ . Since the previous layer is also a capsule layer, the dynamic routing algorithm is used to compute the output. The *background* class was included in the set of  $K$  target events, in order to represent its instance with a dedicated capsule unit and train the system to recognize the absence of events. In the evaluation, however, we consider only the outputs relative to the target sound events. The model predictions are obtained by computing the Euclidean norm of the output of each Detection Capsule. These values represent the probabilities that one of the target events is active in a frame  $t$  of the input feature matrix  $\mathbf{X}$ , thus we consider them as the network output predictions.

In [23], the authors propose a series of densely connected neuron layers stacked at the bottom of the CapsNet, with the aim to regularize the weights training by reconstructing the input image  $\mathbf{X} \in \mathbb{N}^{28 \times 28}$ . Here, this technique entails an excessive complexity of the model to train, due to the higher number of units needed to reconstruct  $\mathbf{X} \in \mathbb{R}^{T \times F \times C}$ , yielding poor performance in our preliminary experiments. We decided, thus, to use dropout [25] and  $L_2$  weight normalization [26] as regularization techniques, as done in [22].

### III. EXPERIMENTAL SET-UP

In order to test the proposed method, we performed a series of experiments on three datasets provided to the participants of different editions of the DCASE challenge [27], [28]. We evaluated the results by comparing the system based on the Capsule architecture with the traditional CNN. The

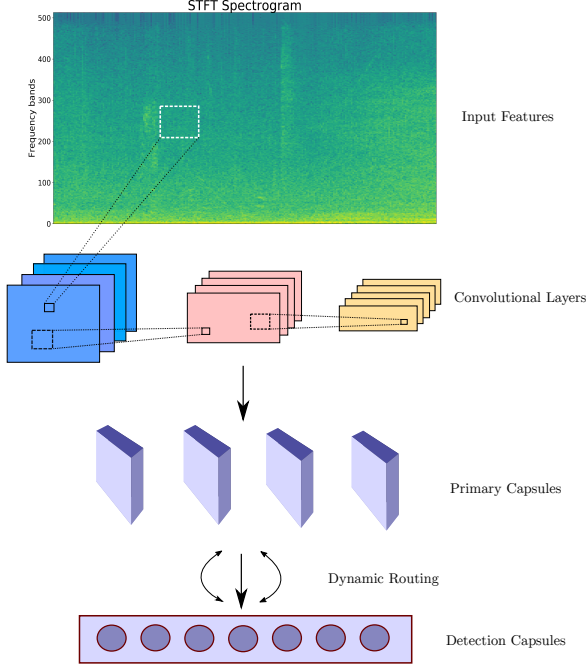


Fig. 1. Flow chart of the Capsule neural network architecture used for polyphonic sound event detection.

hyperparameters of each network have been optimized with a *random search* strategy [29]. Furthermore, we reported the baselines and the best state-of-the-art performance provided by the challenge organizers.

#### A. Dataset

We assessed the proposed method on three datasets, two containing stereo recordings from real-life environments and one artificially generated monophonic mixtures of isolated sound events and real background audio.

In order to evaluate the proposed method in polyphonic real-life conditions, we used the TUT Sound Events 2016 & 2017 datasets, which were included in the corresponding editions of the DCASE Challenge. For the monophonic-SED case study, we used the TUT Rare Sound Events 2017 which represents the task 2 of the DCASE 2017 Challenge.

1) *TUT Sound Events 2016*: The TUT Sound events 2016 (TUT-SED 2016)<sup>1</sup> dataset consists of recordings from two acoustic scenes, respectively “Home” (indoor) and “Residential area” (outdoor) which we considered as two separate subsets. These acoustic scenes were selected from the challenge organizers to represent common environments of interest in applications for safety and surveillance (outside home) and human activity monitoring or home surveillance [28]. A total amount of around 54 and 59 minutes of audio are provided respectively for “Home” and “Residential area” scenarios. Sound events present in each recording were manually annotated without any further cross-verification, due to the high level of subjectivity inherent to the problem. For the “Home” scenario

a total of 11 classes were defined, while for the “Residential Area” scenario 7 classes were annotated.

Each scenario of the TUT-SED 2016 has been divided into two subsets: development dataset and evaluation dataset. The split was done based on the number of examples available for each sound event class. In addition, for the development dataset a cross-validation setup is provided in order to easily compare the results of different approaches on this dataset. The setup consists of 4 folds, so that each recording is used exactly once as test data. In detail, “Residential area” sound events data consists of 5 recordings in the evaluation set and 12 recordings in the development set while “Home” sound events data consists of 5 recordings in the evaluation set and 10 recordings in turn divided into 4 folds as training and validation subsets.

2) *TUT Sound Events 2017*: The TUT Sound Events 2017 (TUT-SED 2017)<sup>2</sup> dataset consists of recordings of street acoustic scenes with various levels of traffic and other activities, for a total of 121 minutes of audio. The scene was selected as representing an environment of interest for detection of sound events related to human activities and hazard situations. It is a subset of the TUT Acoustic scenes 2016 dataset [28], from which also TUT-SED 2016 dataset was taken. Thus, the recording setup, the annotation procedure, the dataset splitting, and the cross-validation setup is the same described above. The 6 target sound event classes were selected to represent common sounds related to human presence and traffic, and they include brakes squeaking, car, children, large vehicle, people speaking, people walking. The evaluation set of the TUT-SED 2017 consists of 29 minutes of audio, whereas the development set is composed of 92 minutes of audio which are employed in the cross-validation procedure.

3) *TUT Rare Sound Events 2017*: The TUT Rare Sound Events 2017 (TUT-Rare 2017)<sup>2</sup> [27] consists of isolated sounds of three different target event classes (respectively, baby crying, glass breaking and gunshot) and 30-second long recordings of everyday acoustic scenes to serve as background, such as park, home, street, cafe, train, etc. [28]. In this case we consider a *monophonic*-SED, since the sound events are artificially mixed with the background sequences without overlap. In addition, the event potentially present in each test file is known a-priori thus it is possible to train different models, each one specialized for a sound event. In the development set, we used a number of sequences equal to 750, 750 and 1250 for training respectively of the baby cry, glass-break and gunshot models, while we used 100 sequences as validation set and 500 sequences as test set for all of them. In the evaluation set, the training and test sequences of the development set are combined into a single training set, while the validation set is the same used in the Development dataset. The system is evaluated against an “unseen” set of 1500 samples (500 for each target class) with a sound event presence probability for each class equal to 0.5.

<sup>1</sup><http://www.cs.tut.fi/sgn/arg/dcase2016/>

<sup>2</sup><http://www.cs.tut.fi/sgn/arg/dcase2017/>

## B. Evaluation Metrics

In this work we used the Error Rate (ER) as primary evaluation metric to ensure comparability with the reference systems. In particular, for the evaluations on the TUT-SED 2016 and 2017 datasets we consider a segment-based ER with a one-second segment length, while for the TUT-Rare 2017 the evaluation metric is event-based error rate calculated using onset-only condition with a collar of 500 ms. In the segment-based ER the ground truth and system output are compared in a fixed time grid, thus sound events are marked as active or inactive in each segment. For the event-based ER the ground truth and system output are compared at event instance level.

ER score is calculated in a single time frame of one second length from intermediate statistics, i.e., the number of substitutions ( $S(t_1)$ ), insertions ( $I(t_1)$ ), deletions ( $D(t_1)$ ) and active sound events from annotations ( $N(t_1)$ ) for a segment  $t_1$ . Specifically:

- 1) Substitutions  $S(t_1)$  are the number of ground truth events for which we have a false positive and one false negative in the same segment;
- 2) Insertions  $I(t_1)$  are events in system output that are not present in the ground truth, thus the false positives which cannot be counted as substitutions;
- 3) Deletions  $D(t_1)$  are events in ground truth that are not correctly detected by the system, thus the false negatives which cannot be counted as substitutions;

These intermediate statistics are accumulated over the segments of the whole test set to compute the evaluation metric ER. Thus, the total error rate is calculated as:

$$ER = \frac{\sum_{t_1=1}^T S(t_1) + \sum_{t_1=1}^T I(t_1) + \sum_{t_1=1}^T D(t_1)}{\sum_{t_1=1}^T N(t_1)}, \quad (9)$$

where  $T$  is the total number of segments  $t_1$ .

If there are multiple scenes in the dataset, such as in the TUT-SED 2016, evaluation metrics are calculated for each scene separately and then the results are presented as the average across the scenes. A detailed and visualized explanation of segment-based ER score in multi label setting can be found in [30].

## C. Comparative Algorithms

Since the datasets we used were employed to develop and evaluate the algorithms proposed from the participants of the DCASE challenges, we can compare our results with the most recent approaches in the state-of-the-art. In addition, each challenge task came along with a baseline method that consists in a basic approach for the SED. It represents a reference for the participants of the challenges while they were developing their systems.

1) *TUT-SED 2016*: The baseline system is based on mel frequency cepstral coefficients (MFCC) acoustic features and multiple GMM-based classifiers. In detail, for each event class, a binary classifier is trained using the audio segments annotated as belonging to the model representing the event class, and the rest of the audio to the model which represents the negative class. The decision is based on likelihood ratio

between the positive and negative models for each individual class, with a sliding window of one second. To the best of our knowledge, the most performing method for this dataset is an algorithm we proposed [31] in 2017, based on binaural MFCC features and a Multi Layer Perceptron (MLP) neural network used as classifier. The detection task is performed by an adaptive energy Voice Activity Detector (VAD) which precedes the MLP and determines the starting and ending point of an event-active audio sequence.

2) *TUT-SED 2017*: In this case the baseline method relies on an MLP architecture using 40 LogMels as audio representation [27]. The network is fed with a feature vector comprehending 5-frame as temporal context. The neural network is composed of two dense layers of 50 hidden units per layer with the 20% of dropout, while the network output layer contains  $K$  sigmoid units (where  $K$  is the number of classes) that can be active at the same time and represent the network prediction of event activity for each context window. The state of the art algorithm is based on the CRNN architecture [32]. The authors compared both monaural and binaural acoustic features, observing that binaural features in general have similar performance as single channel features on the development dataset although the best result on the evaluation dataset is obtained using monaural LogMels as network inputs. According to the authors, this can suggest that the dataset was possibly not large enough to train the CRNN fed with this kind of features.

3) *TUT-Rare 2017*: The baseline [28] and the state-of-the-art methods of the DCASE 2017 challenge (Rare-SED) were based on a very similar architectures to that employed for the TUT-SED 2016 and described above. For the baseline method, the only difference relies in the output layer, which in this case is composed of a single sigmoid unit. The first classified algorithm [33] takes 128 LogMels as input and process them frame-wise by means of a CRNN with 1D filters on the first stage.

## D. Neural Network configuration

We performed a hyperparameter search by running a series of experiments over predetermined ranges. We selected the configuration that leads, for each network architecture, to the best results from the cross-validation procedure on the development dataset of each task, and used this architecture to compute the results on the corresponding evaluation dataset.

The number and shape of convolutional layers, the nonlinear activation function, the regularizers in addition to the capsules dimensions and the maximum number of routing iterations have been varied for a total of 100 configurations. Details of searched hyperparameters and their ranges are reported in Table I. The neural networks training was accomplished by the AdaDelta stochastic gradient-based optimization algorithm [34] for a maximum of 100 epochs and batch size equal to 20 on the margin loss function. The optimizer hyperparameters were set according to [34] (i.e., initial learning rate  $lr = 1.0$ ,  $\rho = 0.95$ ,  $\epsilon = 10^{-6}$ ). The trainable weights were initialized according to the *glorot-uniform* scheme [35] and an early stopping strategy was employed during the training in order to

TABLE I  
HYPERPARAMETERS OPTIMIZED IN THE RANDOM-SEARCH PHASE AND  
THE RESULTING BEST PERFORMING MODELS.

Parameter	Range	Distribution
Batch Normalization	[yes - no]	random choice
CNN layers Nr.	[1 - 4]	uniform
CNN kernels Nr.	[4 - 64]	log-uniform
CNN kernels dim.	[ $3 \times 3$ - $8 \times 8$ ]	uniform
Pooling dim.	[ $1 \times 1$ - $2 \times 5$ ]	uniform
CNN activation	[tanh - relu]	random choice
CNN dropout	[0 - 0.5]	uniform
CNN L2	[yes - no]	random choice
Primary Capsules Nr. $M$	[2 - 8]	uniform
Primary Capsules kernels dim.	[ $3 \times 3$ - $5 \times 5$ ]	uniform
Primary Capsules dimension $J$	[2 - 16]	uniform
Detection Capsules dimension $G$	[2 - 16]	uniform
Capsules dropout	[0 - 0.5]	uniform
Routing iterations	[1 - 5]	uniform

avoid overfitting. If the validation ER did not decrease for 20 consecutive epochs, the training was stopped and the last saved model was selected as the final model. In addition, dropout and  $L_2$  weight normalization (with  $\lambda = 0.01$ ) have been used as weights regularization techniques [25]. The algorithm has been implemented in the Python language using Keras [36] and Tensorflow [37] as deep learning libraries, while Librosa [38] has been used for feature extraction.

For the CNN models, we performed a similar random hyperparameters search procedure for each dataset, considering only the first two blocks of the Table I and by replacing the capsule layers with feedforward layers with *sigmoid* activation function.

On TUT-SED 2016 and 2017 datasets, the event activity probabilities are simply thresholded at a fixed value equal to 0.5, in order to obtain the binary activity matrix used to compute the reference metric. On the TUT-Rare 2017 the network output signal is processed as proposed in [39], thus it is convolved with an exponential decay window then it is processed with a sliding median filter with a local window-size and finally a threshold is applied.

#### IV. RESULTS

In this section, we present the results for all the datasets and experiments described in Section III. The evaluation of Capsule and CNNs based methods have been conducted on the development sets of each examined dataset using random combinations of hyperparameters given in Table I.

##### A. TUT-SED 2016

Results on TUT-SET 2016 dataset are shown in Table III, while Table II reports the configurations which yielded the best performance on the evaluation dataset. All the found models have ReLU as non-linear activation function and use dropout technique as weight regularization, while the batch-normalization applied after each convolutional layer seems to be effective only for the CapsNet. In Table III results are reported considering each combination of architecture and features we evaluated. The best performing setups are highlighted

with bold face. The use of STFT as acoustic representation results to be beneficial for both the architectures with respect to the LogMels. In particular, the CapsNet obtains the lowest ER on the cross-validation performed on Development dataset when is fed by the binaural version of such features. On the two scenarios of the evaluation dataset, a model based on CapsNet and binaural STFT obtains an averaged ER equal to 0.69, which is largely below both the challenge baseline [28] (-0.19) and the best score reported in literature [31] (-0.10). The comparative method based on CNNs seems not to fit at all when LogMels are used as input, while the performance is aligned with the challenge baseline based on GMM classifiers when the models are fed by monaural STFT. This discrepancy can be motivated by the enhanced ability of CapsNet to exploit small training datasets, in particular due to the effect of the routing mechanism on the weight training. In fact, the TUT-SED 2016 is composed of a small amount of audio and the sounds events occur sparsely (i.e., only 49 minutes of the total audio contain at least one event active), thus, the overall results of the comparative methods (CNNs, Baseline and SoA) on this dataset are quite low compared to the other datasets.

Another CapsNet property that is worth to highlight is the lower number of free parameters that compose the models compared to evaluated CNNs. As shown in Table II, the considered architectures have 267K and 252K free parameters respectively for the “Home” and the “Residential area” scenario. It is a relatively low number of parameters to be trained (e.g., a popular deep architecture for image classification such as AlexNet [40] is composed of 60M parameters), and the best performing CapsNets of each considered scenario have even less parameters with respect to the CNNs (-22% and -64% respectively for the “Home” and the “Residential area” scenario). Thus, the high performance of CapsNet can be explained with the architectural advantage rather than the model complexity. In addition, there can be a significant performance shift for the same type of networks with the same number of parameters, which means that a suitable hyperparameters search action (e.g., number of filters on the convolutional layers, dimension of the capsule units) is crucial in finding the best performing network structure.

1) *Closer Look at Network Outputs:* A comparative study on the neural network outputs, which are regarded as event activity probabilities is presented in Fig. 2. The monaural STFT from a 40 seconds sequence of the “Residential area” dataset is shown along with event annotations and the network outputs of the CapsNet and the CNN best performing models. For this example, we chose the monaural STFT as input feature because generally it yields the best results over all the considered datasets. Fig. 2 shows *bird singing* lasting for the whole sequence and correctly detected by both the architectures. When the *car passing by* event overlaps the *bird singing*, the CapsNet detects more clearly its presence. The *people speaking* event is slightly detected by both the models, while the *object banging* activates the relative Capsule exactly only in correspondence of the event annotation. It must be noted that the dataset is composed of unverified manually labelled real-life recordings, that may present a degree of subjectivity, thus, affecting the training. Nevertheless, the

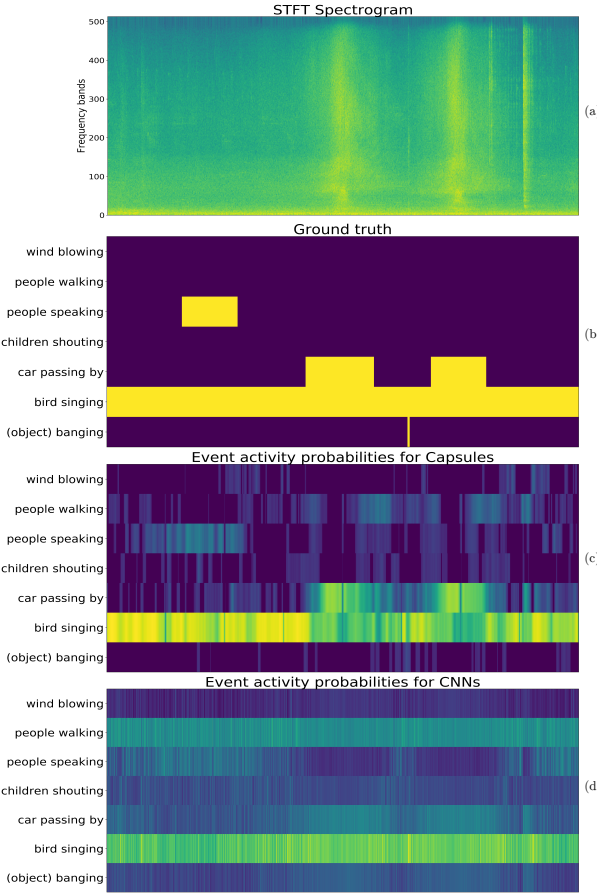


Fig. 2. STFT Spectrogram of the input sequence (a), ground truth (b) and event activity probabilities for CapsNet (c) and CNN (d) from a sequence of test examples from TUT-SED 2016 dataset.

CapsNet exhibits remarkable detection capability especially in the condition of overlapping events, while the CNN outputs are definitely more “blurred” and the event *people walking* is wrongly detected in this sequence.

#### B. TUT-SED 2017

The bottom of Table III reports the results obtained with the TUT-SED 2017. As in the TUT-SED 2016, the best performing models on the Development dataset are those fed by the Binaural STFT of the input signal. In this case we can also observe interesting performance obtained by the CNNs, which on the Evaluation dataset obtain a lower ER (i.e., equal to 0.65) with respect to the state-of-the-art algorithm [32], based on CRNNs. CapsNet confirms its effectiveness and it obtains lowest ER equal to 0.58 with LogMel features, although with a slight margin with respect to the other inputs (i.e., -0.03 compared to the STFT features, -0.06 compared to both the binaural version of LogMels and STFT spectrograms).

It is interesting to notice that in the development cross-validation, the CapsNet models yielded significantly better performance with respect to the other reported approaches, while the CNNs have decidedly worse performance. On the Evaluation dataset, it was not possible to use the early-stopping strategy, thus the ER scores of the CapsNets suffer

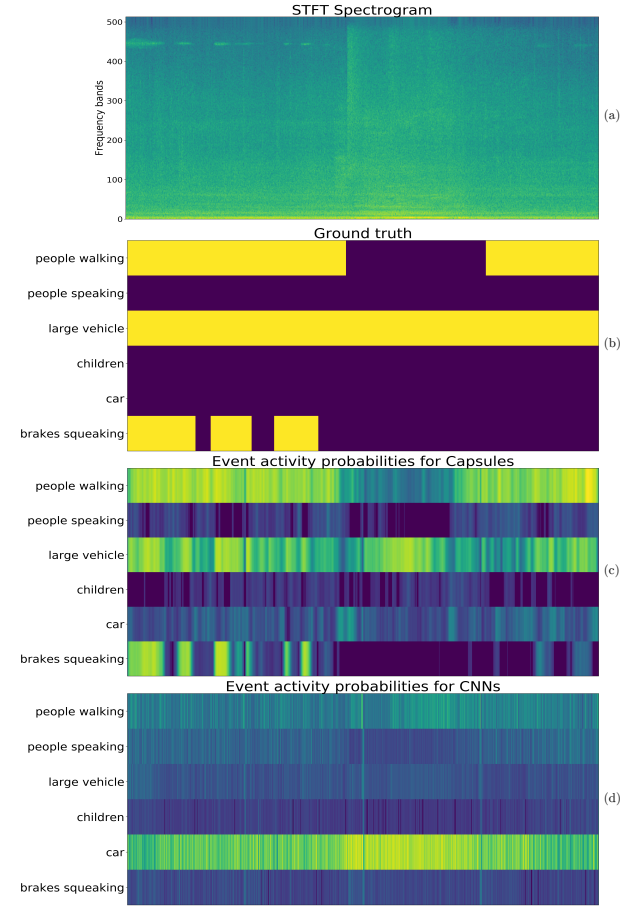


Fig. 3. STFT Spectrogram of the input sequence (a), ground truth (b) and event activity probabilities for CapsNet (c) and CNN (d) from a sequence of test examples from TUT-SED 2017 dataset.

more relative deterioration with respect to the CNNs scores, symptom of the sensibility of the CapsNets to the number of training iterations.

Notwithstanding this weakness, the absolute performance obtained both with monaural and binaural spectral features is consistent and improves the state-of-the-art result, with a reduction of the ER of up to 0.21 in the best case. This is particularly evident in Fig. 3, that shows the output of the two best performing systems for a sequence of approximately 20 seconds length which contains highly overlapping sounds. The event classes “people walking” and “large vehicle” are overlapped for almost all the sequence duration and they are well detected by the CapsNet, although they are of different nature: the “large vehicle” has a typical timber and is almost stationary, while the class “people walking” comprehend impulsive and desultory sounds. The CNN seems not to be able to distinguish between the “large vehicle” and the “car” classes, detecting confidently only the latter, while the activation corresponding “people walking” class is modest. The presence of the “brakes squeaking” class, which has a specific spectral profile mostly located in the highest frequency bands (as shown in the spectrogram), is detected only by the CapsNet. We can assume this as a concrete experimental validation of the routing effectiveness.

TABLE II  
HYPERPARAMETERS OF THE BEST PERFORMING MODELS ON THE TUT-POLYPHONIC SED 2016 & 2017 EVALUATION DATASETS.

	TUT-SED 2016				TUT-SED 2017	
	Home		Residential		Street	
	CapsNet	CNN	CapsNet	CNN	CapsNet	CNN
CNN kernels Nr.	[32, 32, 8]	[64, 64, 16, 64]	[4, 16, 32, 4]	[64]	[4, 16, 32, 4]	[64, 64, 16, 64]
CNN kernels dim.	$6 \times 6$	$5 \times 5$	$4 \times 4$	$5 \times 5$	$4 \times 4$	$5 \times 5$
Pooling dim. ( $F$ axis)	[4, 3, 2]	[2, 2, 2, 2]	[2, 2, 2, 2]	[2]	[2, 2, 2, 2]	[2, 2, 2, 2]
MLP layers dim.	-	[85, 65]	-	[42, 54, 66, 139]	-	[85, 65]
Primary Capsules Nr. $M$	8	-	7	-	7	-
Primary Capsules kernels dim.	$4 \times 4$	-	$3 \times 3$	-	$3 \times 3$	-
Primary Capsules dimension $J$	9	-	16	-	16	-
Detection Capsules dimension $G$	11	-	8	-	8	-
Routing iterations	3	-	4	-	4	-
# Params	267K	343K	252K	709K	223K	342K

TABLE III  
RESULTS OF BEST PERFORMING MODELS IN TERMS OF ER ON THE TUT-SED 2016 & 2017 DATASET.

TUT-SED 2016 - Home									
	Development					Evaluation			
Features	LogMels	Binaural LogMels	STFT	Binaural STFT		LogMels	Binaural LogMels	STFT	Binaural STFT
CNN	11.15	11.58	1.06	1.07		6.80	8.43	0.95	0.92
CapsNet	0.58	0.59	0.44	<b>0.39</b>		0.74	0.75	<b>0.61</b>	0.69
TUT-SED 2016 - Residential Area									
Features	LogMels	Binaural LogMels	STFT	Binaural STFT		LogMels	Binaural LogMels	STFT	Binaural STFT
CNN	3.24	3.11	0.64	1.10		2.36	2.76	1.00	1.35
CapsNet	0.36	0.34	0.32	<b>0.32</b>		0.72	0.75	0.78	<b>0.68</b>
TUT-SED 2016 - Averaged									
CNN	7.20	7.35	0.85	1.09		4.58	5.60	0.98	1.14
CapsNet	0.47	0.47	0.38	<b>0.36</b>		0.73	0.75	0.70	<b>0.69</b>
Baseline [28]			0.91					0.88	
SoA [31]			0.78					0.79	
TUT-SED 2017									
	Development					Evaluation			
Features	LogMels	Binaural LogMels	STFT	Binaural STFT		LogMels	Binaural LogMels	STFT	Binaural STFT
CNN	1.56	2.12	0.57	0.60		1.38	1.79	0.67	0.65
CapsNet	0.45	0.42	<b>0.36</b>	0.36		<b>0.58</b>	0.64	0.61	0.64
Baseline [27]			0.69					0.93	
SoA [32]			0.52					0.79	

The number of free parameters amounts to 223K for the best configuration shown in Table II and it is similar to those found for the TUT-SED 2016, which consists also in this case in a reduction equal to 35% with respect to the best CNN layout.

### C. TUT-Rare SED 2017

The advantage given by the routing procedure to the CapsNet is particularly effective in the case of polyphonic SED. This is confirmed by the results obtained with the TUT-Rare SED 2017 which are shown in Table V. In this case the metric is not anymore segment-based, but it is the event-based ER calculated using onset-only condition. We performed a separate random-search for each of the three sound event

classes both for CapsNets and CNNs and we report the averaged score over the three classes. The setups that obtained the best performance on the Evaluation dataset are shown in Table IV. This is the largest dataset we evaluated and its characteristic is the high unbalance between the amount of background sounds versus the target sound events.

From the analysis of partial results on the Evaluation set (unfortunately not included for the sake of conciseness) we notice that both architectures achieve the best performance on *glass break* sound (0.25 and 0.24 respectively for CNNs and CapsNet with LogMels features), due to its clear spectral fingerprint compared to the background sound. The worst performing class is the *gunshot* (ER equal to 0.58 for the CapsNet), although the noise produced by different instances of this class involves similar spectral components. The low

TABLE IV  
HYPERPARAMETERS OF THE BEST PERFORMING MODELS ON THE TUT-RARE 2017 MONOPHONIC SED EVALUATION DATASETS.

TUT-Rare SED 2017 Monophonic SED					
	Babycry		Glassbreak		Gunshot
	CapsNet	CNN	CapsNet	CNN	CapsNet
CNN kernels Nr.	[16, 64, 32]	[16, 32, 8, 16]	[16, 64, 32]	[16, 32, 8, 16]	[16, 16]
CNN kernels dim.	$6 \times 6$	$8 \times 8$	$6 \times 6$	$8 \times 8$	$8 \times 8$
Pooling dim. ( $F$ axis)	[4, 3, 2]	[3, 3, 2, 2]	[4, 3, 2]	[3, 3, 2, 2]	[5, 2]
MLP layers dim.	-	[212, 67]	-	[212, 67]	-
Primary Capsules Nr. $M$	7	-	7	-	8
Primary Capsules kernels dim.	$3 \times 3$	-	$3 \times 3$	-	$3 \times 3$
Primary Capsules dimension $J$	8	-	8	-	8
Detection Capsules dimension $G$	14	-	14	-	6
Routing iterations	5	-	5	-	1
# Params	131K	84K	131K	84K	30K
					211K

performance is probably motivated due to the fast decay of this sound, which means that in this case the routing procedure is not sufficient to avoid confusing the *gunshot* with other background noises, especially in the case of dataset unbalancing and low event-to-background ratio. A solution to this issue can be find in the combination of CapsNet with RNN units, as proposed in [19] for the CNNs which yields an efficient modelling of the *gunshot* by CRNN and improves the detection abilities even in polyphonic conditions. The *babycry* consists of short, harmonic sounds is detected almost equally from the two architectures due to the property of frequency shift invariance given by the convolutional kernel processing.

Finally, the CNN shows better generalization performance to the CapsNet, although the ER score is far from state-of-the-art which involves the use of the aforementioned CRNNs [33] or a hierarchical framework [39]. In addition, in this case are the CNN models to have a reduced number of weights to train (36%) with respect the CapsNets, except for the “*gunshot*” case but, as mentioned, it is also the configuration that gets the worst results.

TABLE V  
RESULTS OF BEST PERFORMING MODELS IN TERMS OF ER ON THE TUT-RARESED 2017 DATASET.

TUT-RareSED 2017 - Monophonic SED				
	Development		Evaluation	
Features	LogMels	STFT	LogMels	STFT
CNN	0.29	0.21	<b>0.41</b>	0.46
CapsNet	<b>0.17</b>	0.20	0.45	0.54
Baseline [28]	0.53		0.64	
Hierarchic CNNs [39]	0.13		0.22	
SoA [33]	<b>0.07</b>		<b>0.13</b>	

#### D. Alternative Dynamic Routing for SED

We observed that the original routing procedure implies the initialization of the coefficients  $\beta_{ij}$  to zero each time the procedure is restarted, i.e., after each input sample has been processed. This is reasonable in the case of image classification, for which the CapsNet has been originally proposed. In the case of audio task, we clearly expect a higher

TABLE VI  
RESULTS OF TEST PERFORMED WITH OUR PROPOSED VARIANT OF ROUTING PROCEDURE.

TUT-SED 2016 - Home			
	Development	Evaluation	
CapsNet	0.44		0.61
CapsNet - NR	0.41	-6.8 %	<b>0.58</b> -4.9 %
TUT-SED 2016 - Residential			
CapsNet	0.32		0.78
CapsNet - NR	0.31	-3.1 %	<b>0.72</b> -7.7 %
TUT-SED 2016 - Average			
CapsNet	0.38		0.70
CapsNet - NR	0.36	-5.3 %	<b>0.65</b> -7.1 %
TUT-SED 2017 - Street			
CapsNet	0.36		0.61
CapsNet - NR	0.36	-0.0 %	<b>0.58</b> -4.9 %

correlation between samples belonging to adjacent temporal frames  $\mathbf{X}$ . We thus investigated the chance to initialize the coefficients  $\beta_{ij}$  to zero only at the very first iteration, while for subsequent  $\mathbf{X}$  to assign them the last values they had at the end of the previous iterative procedure. We experimented this variant considering the best performing models of the analyzed scenarios for polyphonic SED, taking into account only the systems fed with the monaural STFT. As shown in Table VI, the modification we propose in the routing procedure is effective in particular on the evaluation datasets, conferring improved generalization properties to the models we tested even without accomplishing a specific hyperparameters optimization.

## V. CONCLUSION

In this work, we proposed to apply a novel neural network architecture, the CapsNet, to the polyphonic SED task. The architecture is based on both convolutional and capsule layers. The convolutional layers extract high-level time-frequency feature maps from input matrices which provide an acoustic spectral representation with long temporal context. The obtained feature maps are then used to feed the Primary Capsule

layer which is connected to the Detection Capsule layer, finally extracting the event activity probabilities. These last two layers are involved in the iterative *routing-by-agreement* procedure, which computes the outputs based on a measure of likelihood between a capsule and its parent capsules. This architecture combines, thus, the ability of convolutional layers to learn local translation invariant filters with the ability of capsules to learn part-whole relations by using the routing procedure.

Part of the novelty of this work resides in the adaptation of the CapsNet architecture for the audio event detection task, with a special care on the input data, the layers interconnection and the regularization techniques. The routing procedure is also modified to confer a more appropriate acoustic rationale, with a further average performance improvement of 6% among the polyphonic-SED tasks.

An extensive evaluation of the algorithm is proposed with comparison to recent state-of-the-art methods on three different datasets. The experimental results demonstrate that the use of dynamic routing procedure during the training is effective and provides significant performance improvement in the case of overlapping sound events compared to traditional CNNs, and other established methods in polyphonic SED. Interestingly, the CNN based method obtained the best performance in the monophonic SED case study, thus emphasizing the suitability of the CapsNet architecture in dealing with overlapping sounds. We showed that this model is particularly effective with small sized datasets, such as TUT-SED 2016 which contains a total 78 minutes of audio for the development of the models of which one third is background noise.

Furthermore, the network trainable parameters are reduced with respect to other deep learning architectures, confirming the architectural advantage given by the introduced features also in the task of polyphonic SED.

Despite the improvement in performance, we identified a limitation of the proposed method. As presented in Section IV, the performance of the CapsNet is more sensible to the number of training iterations. This affects the generalization capabilities of the algorithm, yielding a greater relative deterioration of the performance on evaluation datasets with respect to the comparative methods.

The results we observed in this work are consistent with many other classification tasks in various domains [41]–[43], prove that the CapsNet is an effective approach which enhances the well-established representation capabilities of the CNNs also in the audio field. As a future work, regularization methods can be investigated to overcome the lack of generalization which seems to affect the CapsNets. Furthermore, regarding the SED task the addition of recurrent units may be explored to enhance the detection of particular (i.e., impulsive) sound events in real-life audio and the recently-proposed variant of routing, based on the Expectation Maximization algorithm (EM) [44], can be investigated in this context.

#### ACKNOWLEDGEMENT

This research has been partly supported by the Italian University and Research Consortium CINECA. We acknowledge them for the availability of high performance computing resources and support.

#### REFERENCES

- [1] T. Virtanen, M. D. Plumley, and D. Ellis, *Computational analysis of sound scenes and events*. Springer, 2018.
- [2] M. Crocco, M. Cristani, A. Trucco, and V. Murino, “Audio surveillance: a systematic review,” *ACM Computing Surveys (CSUR)*, vol. 48, no. 4, p. 52, 2016.
- [3] Y.-T. Peng, C.-Y. Lin, M.-T. Sun, and K.-C. Tsai, “Healthcare audio event classification using hidden Markov models and hierarchical hidden Markov models,” in *Proc. of ICME*, 2009.
- [4] P. Foggia, N. Petkov, A. Saggese, N. Strisciuglio, and M. Vento, “Reliable detection of audio events in highly noisy environments,” *Pattern Recognition Letters*, vol. 65, pp. 22–28, 2015.
- [5] J. Salamon and J. P. Bello, “Deep convolutional neural networks and data augmentation for environmental sound classification,” *IEEE Signal Processing Letters*, vol. 24, no. 3, pp. 279–283, 2017.
- [6] T. Grill and J. Schlter, “Two convolutional neural networks for bird detection in audio signals,” in *Proc. of EUSIPCO*. IEEE, Aug 2017, pp. 1764–1768.
- [7] D. Stowell and D. Clayton, “Acoustic event detection for multiple overlapping similar sources,” in *Proc. of WASPAA*. IEEE, 2015, pp. 1–5.
- [8] N. Degara, M. E. Davies, A. Pena, and M. D. Plumley, “Onset event decoding exploiting the rhythmic structure of polyphonic music,” *IEEE J. Sel. T. in Signal Proc.*, vol. 5, no. 6, pp. 1228–1239, 2011.
- [9] T. Heittola, A. Mesaros, A. Eronen, and T. Virtanen, “Audio context recognition using audio event histograms,” in *Proc. of EUSIPCO*, 2010, pp. 1272–1276.
- [10] J. J. Carabias-Orti, T. Virtanen, P. Vera-Candeas, N. Ruiz-Reyes, and F. J. Canadas-Quesada, “Musical instrument sound multi-excitation model for non-negative spectrogram factorization,” *IEEE J. Sel. T. in Signal Proc.*, vol. 5, no. 6, pp. 1144–1158, 2011.
- [11] G. Guo and S. Z. Li, “Content-based audio classification and retrieval by support vector machines,” *IEEE Trans. Neural Netw.*, vol. 14, no. 1, pp. 209–215, 2003.
- [12] I. McLoughlin, H. Zhang, Z. Xie, Y. Song, and W. Xiao, “Robust sound event classification using deep neural networks,” *IEEE Trans. Audio, Speech, Language Process.*, vol. 23, no. 3, pp. 540–552, 2015.
- [13] A.-r. Mohamed, G. E. Dahl, G. Hinton *et al.*, “Acoustic modeling using deep belief networks,” *IEEE Trans. Audio, Speech, Language Process.*, vol. 20, no. 1, pp. 14–22, 2012.
- [14] K. J. Piczak, “Environmental sound classification with convolutional neural networks,” in *Proc. of MLSP*. IEEE, 2015, pp. 1–6.
- [15] A. Graves, A.-r. Mohamed, and G. Hinton, “Speech recognition with deep recurrent neural networks,” in *Proc. of ICASSP*. IEEE, 2013, pp. 6645–6649.
- [16] G. Trigeorgis, F. Ringeval, R. Brueckner, E. Marchi, M. A. Nicolaou, B. Schuller, and S. Zafeiriou, “Adieu features? end-to-end speech emotion recognition using a deep convolutional recurrent network,” in *Proc. of ICASSP*. IEEE, 2016, pp. 5200–5204.
- [17] B. Wu, K. Li, F. Ge, Z. Huang, M. Yang, S. M. Siniscalchi, and C.-H. Lee, “An end-to-end deep learning approach to simultaneous speech dereverberation and acoustic modeling for robust speech recognition,” *IEEE J. Sel. T. in Signal Proc.*, vol. 11, no. 8, pp. 1289–1300, 2017.
- [18] M. Espi, M. Fujimoto, K. Kinoshita, and T. Nakatani, “Exploiting spectro-temporal locality in deep learning based acoustic event detection,” *EURASIP J. on Audio, Speech, and Music Process.*, vol. 2015, no. 1, p. 26, Sep 2015.
- [19] E. Cakir, G. Parascandolo, T. Heittola, H. Huttunen, and T. Virtanen, “Convolutional recurrent neural networks for polyphonic sound event detection,” *IEEE Trans. Audio, Speech, Language Process.*, vol. 25, no. 6, pp. 1291–1303, 2017.
- [20] T. Virtanen, A. Mesaros, T. Heittola, A. Diment, E. Vincent, E. Benetos, and B. M. Elizalde, *Proceedings of the Detection and Classification of Acoustic Scenes and Events 2017 Workshop*. Tampere University of Technology, Laboratory of Signal Processing, 2017.
- [21] F. Vesperini, L. Gabrielli, E. Principi, and S. Squartini, “A capsule neural networks based approach for bird audio detection,” Ancona, Italy, 2018, DCASE Tech. Report. Copyright-free.
- [22] T. Iqbal, Y. Xu, Q. Kong, and W. Wang, “Capsule routing for sound event detection,” in *Proc. of EUSIPCO*. IEEE, Sept. 3–7 2018.
- [23] S. Sabour, N. Frosst, and G. E. Hinton, “Dynamic routing between capsules,” in *Advances in Neural Information Processing Systems*, 2017, pp. 3856–3866.
- [24] G. E. Hinton, A. Krizhevsky, and S. D. Wang, “Transforming auto-encoders,” in *Proc. of ICANN*. Springer, 2011, pp. 44–51.

- [25] N. Srivastava, G. Hinton, A. Krizhevsky, I. Sutskever, and R. Salakhutdinov, "Dropout: A simple way to prevent neural networks from overfitting," *J. of Machine Learning Research*, vol. 15, no. 1, pp. 1929–1958, 2014.
- [26] A. E. Hoerl and R. W. Kennard, "Ridge regression: Biased estimation for nonorthogonal problems," *Technometrics*, vol. 12, no. 1, pp. 55–67, 1970.
- [27] A. Mesaros, T. Heittola, A. Diment, B. Elizalde, A. Shah, E. Vincent, B. Raj, and T. Virtanen, "DCASE 2017 challenge setup: Tasks, datasets and baseline system," in *Proc. of DCASE*, 2017.
- [28] A. Mesaros, T. Heittola, and T. Virtanen, "TUT database for acoustic scene classification and sound event detection," in *Proc. of EUSIPCO*, Aug 2016, pp. 1128–1132.
- [29] J. Bergstra and Y. Bengio, "Random search for hyper-parameter optimization," *J. of Machine Learning Research*, vol. 13, no. Feb, pp. 281–305, 2012.
- [30] A. Mesaros, T. Heittola, and T. Virtanen, "Metrics for polyphonic sound event detection," *Applied Sciences*, vol. 6, no. 6, p. 162, 2016.
- [31] M. Valenti, D. Tonelli, F. Vesperini, E. Principi, and S. Squartini, "A neural network approach for sound event detection in real life audio," in *Proc. of EUSIPCO*. IEEE, 2017, pp. 2754–2758.
- [32] S. Adavanne and T. Virtanen, "A report on sound event detection with different binaural features," *arXiv preprint arXiv:1710.02997*, 2017.
- [33] H. Lim, J. Park, and Y. Han, "Rare sound event detection using 1D convolutional recurrent neural networks," in *Proc. of DCASE*, 2017, pp. 80–84.
- [34] M. D. Zeiler, "AdaDelta: an adaptive learning rate method," *arXiv preprint arXiv:1212.5701*, 2012.
- [35] X. Glorot and Y. Bengio, "Understanding the difficulty of training deep feedforward neural networks," in *Proc. of AISTATS*, 2010, pp. 249–256.
- [36] F. Chollet *et al.*, "Keras," <https://github.com/keras-team/keras>, 2015.
- [37] M. Abadi *et al.*, "TensorFlow: Large-scale machine learning on heterogeneous systems," pp. 265–283, 2016. [Online]. Available: <https://www.tensorflow.org/>
- [38] B. McFee, C. Raffel, D. Liang, D. P. Ellis, M. McVicar, E. Battenberg, and O. Nieto, "librosa: Audio and music signal analysis in python," in *Proc. of SciPy*, 2015, pp. 18–25.
- [39] F. Vesperini, D. Drogolini, E. Principi, L. Gabrielli, and S. Squartini, "Hierarchic ConvNets framework for rare sound event detection," in *Proc. of EUSIPCO*. IEEE, Sept. 3–7 2018.
- [40] A. Krizhevsky, I. Sutskever, and G. E. Hinton, "Imagenet classification with deep convolutional neural networks," in *Advances in neural information processing systems*, 2012, pp. 1097–1105.
- [41] F. Deng, S. Pu, X. Chen, Y. Shi, T. Yuan, and S. Pu, "Hyperspectral image classification with capsule network using limited training samples," *Sensors*, vol. 18, no. 9, 2018.
- [42] Y. Shen and M. Gao, "Dynamic routing on deep neural network for thoracic disease classification and sensitive area localization," in *Machine Learning in Medical Imaging*, Y. Shi, H.-I. Suk, and M. Liu, Eds. Springer International Publishing, 2018, pp. 389–397.
- [43] M. A. Jalal, R. Chen, R. K. Moore, and L. Mihaylova, "American sign language posture understanding with deep neural networks," in *Proc. of FUSION*. IEEE, 2018, pp. 573–579.
- [44] G. E. Hinton, S. Sabour, and N. Frosst, "Matrix capsules with EM routing," in *Proc. of ICLR*, Vancouver, BC, 2018.



**Leonardo Gabrielli** got his M.Sc. and PhD degrees in Electronics Engineering from Università Politecnica delle Marche, Italy, respectively in 2011 and 2015. His main research topics are related to audio signal processing and machine learning with application to sound synthesis, Computational Sound Design, Networked Music Performance, Music Information Retrieval and audio classification. He has been co-founder of DowSee srl, and holds several industrial patents. He is coauthor of more than 30 scientific papers.



**Emanuele Principi** was born in Senigallia (Ancona), Italy, on January 1978. He received the M.S. degree in electronic engineering (with honors) from Università Politecnica delle Marche (Italy) in 2004. He received his Ph.D. degree in 2009 in the same university under the supervision of Prof. Francesco Piazza. In November 2006 he joined the 3MediaLabs research group coordinated by Prof. Francesco Piazza at Università Politecnica delle Marche where he collaborated to several regional and european projects on audio signal processing. Dr. Principi is author and coauthor of several international scientific peer-reviewed articles in the area of speech enhancement for robust speech and speaker recognition and intelligent audio analysis. He is member of the IEEE CIS Task Force on Computational Audio Processing, and is reviewer for several international journals. His current research interests are in the area of machine learning and digital signal processing for the smart grid (energy task scheduling, non-intrusive load monitoring, computational Intelligence for vehicle to grid) and intelligent audio analysis (multi-room voice activity detection and speaker localization, acoustic event detection, fall detection).



**Stefano Squartini** (IEEE Senior Member, IEEE CIS Member) was born in Ancona, Italy, on March 1976. He got the Italian Laurea with honors in electronic engineering from University of Ancona (now Polytechnic University of Marche, UnivPM), Italy, in 2002. He obtained his PhD at the same university (November 2005). He worked also as post-doctoral researcher at UnivPM from June 2006 to November 2007, when he joined the DII (Department of Information Engineering) as Assistant Professor in Circuit Theory. He is now Associate Professor at UnivPM since November 2014. His current research interests are in the area of computational intelligence and digital signal processing, with special focus on speech/audio/music processing and energy management. He is author and coauthor of more than 190 international scientific peer-reviewed articles. He is Associate Editor of the IEEE Transactions on Neural Networks and Learning Systems, IEEE Transactions on Cybernetics and IEEE Transactions on Emerging Topics in Computational Intelligence, and also member of Cognitive Computation, Big Data Analytics and Artificial Intelligence Reviews Editorial Boards. He joined the Organizing and the Technical Program Committees of more than 70 International Conferences and Workshops in the recent past. He is the Organizing Chair of the IEEE CIS Task Force on Computational Audio Processing.



**Fabio Vesperini** was born in San Benedetto del Tronto, Italy, on May 1989. He received his M.Sc. degree (cum laude) in electronic engineering in 2015 from Università Politecnica delle Marche (UnivPM). In 2014 he was at the Technische Universität München as visiting student for 7 months, where he carried out his master thesis project on acoustic novelty detection. He is currently a PhD student at the Department of Information Engineering, at UnivPM. His research interests are in the fields of digital signal processing and machine learning for intelligent audio analysis.